Yonago Acta medica 1996;39:163–170

Assessment of the Image Quality and Tumor Detectability of Breath-Hold T2-Weighted Imaging of Liver Tumors using a Fast Gradient MR System

Kotaro Yoshida, Yuji Suto, Shuji Sugihara and Yukiko Tokuda

Department of Radiology, Faculty of Medicine, Tottori University, Yonago 683, Japan

Fourteen patients with various types of focal liver tumors were imaged with turbo spin-echo (TSE), breath-hold TSE (BH-TSE) and half-Fourier single-shot TSE (HASTE) pulse sequences using a fast gradient magnetic resonance imaging (MRI) system. We compared the T2-weighted images of the liver with the TSE, BH-TSE, HASTE and conventional spin-echo (SE) pulse sequences in order to determine whether those fast T2-weighted images, including fat suppressed images, could replace SE images. In quantitative and qualitative analysis, the fast T2-weighted images were slightly superior to the SE images, but they were inferior in the conspicuousness of liver tumor to the SE images. These findings suggest that the fast T2-weighted images can shorten the examination time of the liver MRI, but cannot replace the T2-weighted SE images because of the low conspicuousness.

Key words: breath-hold MRI; fast gradient; T2-weighted image; liver tumor

Magnetic resonance imaging (MRI), especially in T2-weighted images, has been reported to have an excellent contrast resolution and to be useful in detection and diagnosis of tumorous lesions of the liver (Rammeny et al., 1989; Egglin et al., 1990). However, by the conventional spin-echo (SE) method, a long examination time is needed for scanning, and deterioration of the image quality due to various artifacts including respiratory artifacts has been a problem (Wood et al., 1988). Recently, however, whole liver imaging with breath-holding has become possible by both T1-weighted and T2-weighted images due to the development of various fast imaging methods and increased availability of the fast gradient MRI systems (Winkler et al., 1989; Siewert et al., 1994).

We previously reported that the breath-hold T1-weighted imaging by the gradient-echo method shortened the time needed for the examination and was more useful than the SE method for detection and diagnosis of liver tumors (Yoshida et al., 1996).

In this study, we quantitatively and qualitatively compared the image quality and the detectability of liver tumors by images of the T2-weighted SE (SET2) and various fast sequences. The fast sequences were the turbo SE (TSE) method with breathing at rest, breath-hold TSE method (BH-TSE) and half-Fourier single-shot TSE method (HASTE) with a faster examination speed and heavier T2-weighted image than ordinary TSE (Hening et al., 1986; Fujii, 1994). We also compared their fat saturation (fs) images with those by SET2 and examined whether these breath-hold T2-weighted imaging techniques can replace SET2.

Abbreviations: BH-TSE, breath-hold TSE; CNR, contrast-to-noise ratio; CNR_{SP}, spleen-liver CNR; CNR_T, tumor-liver CNR; FOV, field of view; fs, fat saturation; HASTE, half-Fourier single-shot TSE; MRI, magnetic resonance imaging; MTC, magnetization transfer contrast; ROI, regions of interest; SE, spin-echo; SET2, T2-weighted SE; SI, signal intensity; SD_{BKG}, SD of background; SI_L, SI of the liver; SI_{SP}, SI of the spleen; SI_T, SI of the tumor; SNR, signal-to-noise ratio; TE, echo time; TR, repetition time; TSE, turbo SE

Table 1. Imaging parameters of each pulse sequence

Parameter	Sequence			
	SET2	TSE	BH-TSE	HASTE
Repetition time (ms)	1800	3500	4500	10.9
Echo time (ms)	80	99	138	87
Echo train length		11	29	128
No. of acquisitions	2	5	1	1
Matrix size	157×256	176×256	116×256	128×256
Imaging time	9 min 28 s	4 min 43 s	23 s	12 s

BH-TSE, breath-hold TSE; HASTE, half-Fourier single-shot TSE; SET2, conventional T2 weighted spin-echo; TSE, turbo spin-echo.

Subjects and Methods

The subjects were 14 patients with 42 tumorous lesions of the liver (11 males and 3 females ranging in age from 33 to 83 years, mean 63.5 years) who underwent MRI between June, 1995 and March, 1996. The lesions were 31 nodes of hepatocellular carcinoma, 6 nodes of metastatic liver tumor, and 5 nodes of liver cysts diagnosed on the basis of the clinical findings and image findings. Quantitative evaluation was made in 26 nodes detected by SET2, TSE, BH-TSE, HASTE and their fs images, and qualitative evaluation was made in 42 nodes detected by anyone of these imaging methods. The masses were 0.6–10.5 cm (mean 3.8 cm) in diameter.

A 1.5 T fast gradient superconducting MRI system (Magnetom Vision: Siemens, Erlangen, Germany, maximum gradient magnetic field intensity 25 mT/m) was used. A phased array coil was used in all patients. Table 1 shows imaging conditions. The fs images were obtained with the same parameters using frequency-selective saturation pulses (Haase et al., 1985; Hata and Tada, 1994). Transaxial images at a slice thickness of 10 mm, a gap of 1 mm and a field of view (FOV) of 35–42 cm were obtained. A rectangular FOV with a 6/8 of 7/8 phase encode reduction was used depending on the body, and a presaturation pulse was impressed at the upper and lower ends of the imaging region.

Quantitative evaluation was made by determining the region-of-interest (ROI) over the liver, spleen and solid part of the tumor as widely as possible and by avoiding blood vessels in each imaging method. Also, ROI was determined as widely as possible over the background on the abdominal side of each patient, which was the phase encoding direction. Each ROI was 35 pixels or wider, and the mean signal intensity (SI) and SD per pixel of liver (SI_L), spleen (SI_{SP}), tumor (SI_T) and background (SD_{BKG}) were calculated. The signal-to-noise ratio (SNR) of the liver, spleen-liver contrast-to-noise ratio (CNR_{SP}) and tumor-liver contrast-to-noise ratio (CNR_T) were calculated as follows: $SNR = SI_L/SD_{BKG}$, $CNR_{SP} = (SI_{SP} - SI_L)/SD_{BKG}$, $CNR_T = (SI_T - SI_L)/SD_{BKG}$. The results of SET2 and fast imaging methods were compared with Student's *t*-test when the variance was equal and by Welch's *t*-test when the variance was unequal.

Qualitatively, each image was evaluated by the following 6 items: i) motion artifacts by breathing and vascular pulsation, ii) liver-spleen and liver-tumor contrast, iii) visibility of intrahepatic vessels, iv) visibility of tumor structures (margin, septum, capsule), v) sharpness of the liver margin and vi) overall image quality, taking into consideration the assessments in i) to vi). The assessments done by 3 radiologists were numerically represented in the following 5 grades and numerical rating: poor (1 point); fair (2 points); moderate (3 points); good (4 points); or excellent (5 points). Based on this numerical rating, comparative evaluation of the quality of each image was made with the Wilcoxon matched-pairs signed-rank test. In addition, the number of nodes

visualized by each image was compared according to the diameter of the nodes (less than 1 cm, 1 cm or larger, less than 2 cm, 2 cm or larger, less than 3 cm and 3 cm or larger).

Results

Table 2 shows the results of the quantitative evaluation. The SNR of the liver was significantly higher in TSEfs ($P < 0.05$) and HASTE ($P < 0.01$) than in SET2 or TSE. No significant differences were observed among the other fast imaging techniques. The CNR_{SP} showed no significant difference be tween SET2 and fast imaging methods with and without breath-holding. The CNR_T was significantly higher in HASTE ($P < 0.05$) and HASTEfs ($P < 0.01$) than in SET2 and in TSEfs ($P < 0.01$). It was also significantly higher in HASTE ($P < 0.05$), and HASTEfs ($P < 0.01$) than in TSE.

Figure 1 shows the results of the qualitative image evaluation. Respiratory artifacts were greater in TSE ($P < 0.05$) but were significantly smaller in TSEfs ($P < 0.05$), HASTE ($P < 0.01$) and HASTEfs ($P < 0.05$) than in SET2. Vascular artifacts were greater in BH-TSEfs ($P < 0.05$) but were significantly smaller in TSEfs ($P < 0.05$), HASTE ($P < 0.05$) and HASTEfs ($P < 0.05$). Liver-tumor contrast was significantly better in TSEfs ($P < 0.01$) and BH-TSEfs ($P < 0.05$), and liver-spleen contrast was significantly better in TSEfs ($P < 0.01$). In the visibility of tumor structures, the information concerning the capsule and the internal structure such as the mosaic structure was richer in TSE ($P < 0.05$), TSEfs ($P < 0.01$), BH-TSEfs ($P < 0.05$) and HASTEfs ($P < 0.05$). The visibility of intrahepatic vessels was inferior in TSEfs ($P < 0.05$). The sharpness of the liver margin was superior in TSE ($P < 0.05$), and BH-TSE and BH-TSEfs ($P < 0.01$). The overall image quality was better in TSEfs ($P < 0.05$) than in SET2 but was not significantly different in other methods. Figure 2 shows a case of hepatocellular carcinoma in the left hepatic lobe.

Table 3 compares the number of tumors detected by each image. Tumors of all sizes were detected most clearly in SET2 except that a hepatocellular carcinoma of 3.5 cm in diameter located in the lower margin of the liver was not visible.

Discussion

Various fast T2-weighted MRI techniques have been developed, and the imaging time was shortened in the central nervous system, head and neck, and pelvic regions (Feinberg and Oshio, 1991; Jones et al., 1992; Nghiem et al., 1992). In the abdominal region, however, respiratory artifacts cannot be reduced by shortening of the imaging time, and the problem of image deterioration due to respiratory movements has remained (Stalk et al., 1987). However, T2-

Table 2. Results of quantitative evaluation in each imaging sequence

Sequence	Parameter			
	Liver SNR	Contrast	CNR_T	CNR_{SP}
SET2	10.1 ± 3.6	0.30 ± 0.13	11.3 ± 7.5	14.2 ± 4.4
TSE	7.6 ± 3.4	0.37 ± 0.13	8.5 ± 4.4	11.4 ± 5.5
TSEfs	17.0 ± 4.1*††	0.37 ± 0.14	21.8 ± 12.2††	19.4 ± 10.5
BH-TSE	6.8 ± 2.7	0.43 ± 0.20	15.7 ± 14.1	12.1 ± 4.5
BH-TSEfs	8.3 ± 2.8	0.45 ± 0.17*	17.2 ± 13.4	14.9 ± 4.5
HASTE	15.4 ± 7.4	0.35 ± 0.21	51.8 ± 55.6*†	14.5 ± 10.7
HASTEfs	24.9 ± 7.3**††	0.40 ± 0.20	32.9 ± 18.7**††	23.3 ± 16.3

CNR_{SP}, spleen-to-liver contrast-to-noise ratio; CNR_T: tumor-to-liver CNR; fs, fat-saturation; SNR, signal-to-noise ratio. The other abbreviations are the same as in Table 1.

* $P < 0.05$, ** $P < 0.01$ to SET2.

† $P < 0.05$, †† $P < 0.01$ to TSE.

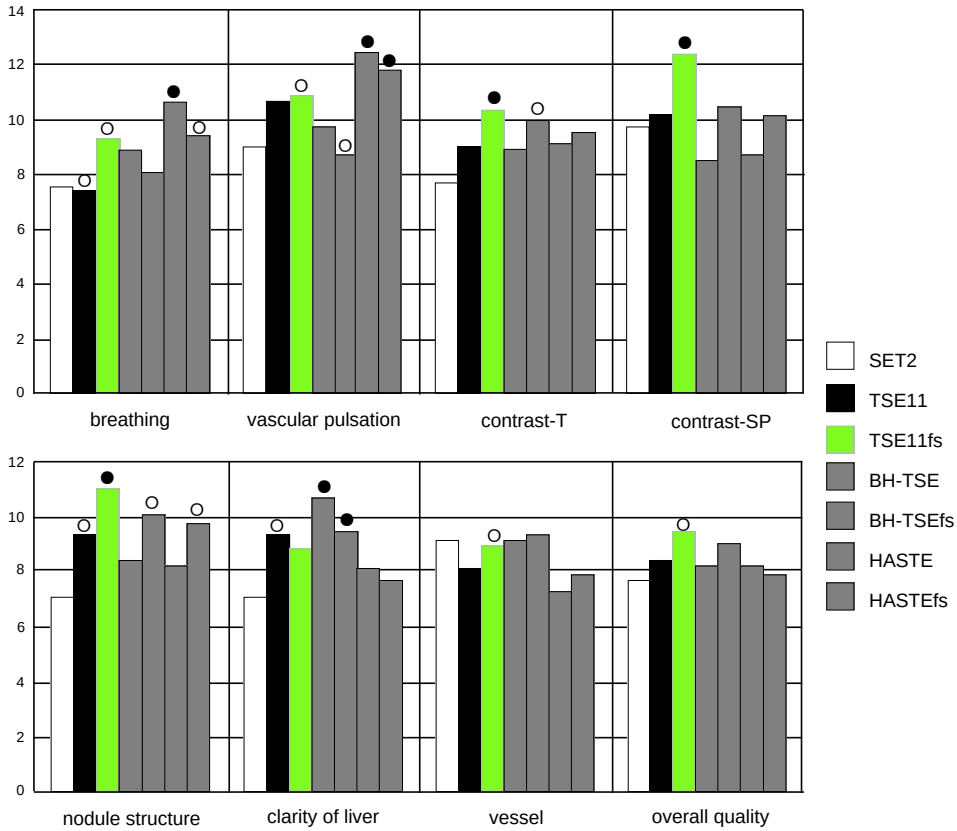

Fig. 1. Qualitative assessment of the image quality on fast, chemical fat-saturation (fs) fast and conventional T2-weighted spin-echo (SE) magnetic resonance (MR) images (○ $P < 0.05$, ● $P < 0.01$). Respiratory artifacts were greater in turbo SE (TSE) ($P < 0.05$) but were significantly smaller in TSEfs ($P < 0.05$), half-Fourier single-shot TSE (HASTE) ($P < 0.01$) and HASTEfs ($P < 0.05$) than in T2-weighted SE (SET2). Vascular artifacts were greater in breath-hold TSE fs (BH-TSEfs) ($P < 0.05$) but were significantly smaller in TSEfs ($P < 0.05$), HASTE ($P < 0.05$) and HASTEfs ($P < 0.05$). Liver-tumor contrast was significantly better in TSEfs ($P < 0.01$) and BH-TSEfs ($P < 0.05$), and liver-spleen contrast was significantly better in TSEfs ($P < 0.01$). In the visibility of tumor structures, the information concerning the capsule and the internal structure such as the mosaic structure was richer in TSE ($P < 0.05$), TSEfs ($P < 0.01$), BH-TSEfs ($P < 0.05$) and HASTEfs ($P < 0.05$). The visibility of intrahepatic vessels was inferior in TSEfs ($P < 0.05$). The sharpness of the liver margin was superior in TSE ($P < 0.05$), and BH-TSE and BH-TSEfs ($P < 0.01$). The overall image quality was better in TSEfs ($P < 0.05$) than in SET2 but was not significantly different in other methods.

weighted imaging methods with breath-holds such as TSE and HASTE have become possible due to recent improvements in the instrument (Winkler et al., 1989; de Lange et al., 1994; Taupitz et al., 1995; Rydberg et al., 1995).

By TSE, T2-weighted images can be obtained in a shorter time than SE by phase-encoding of each echo obtained by several 180 pulses per excitation pulse. By HASTE, an accelerated version of TSE, one image can be obtained in

Fig. 2 (opposite page). MR images for a 76-year-old patient with hepatocellular carcinoma (arrows). The SET2 (**A**), TSE (**B**), TSEfs (**C**), BH-TSE (**D**), BH-TSEfs (**E**), HASTE (**F**) and HASTEfs (**G**) images show hepatocellular carcinoma in the left hepatic lobe. The contrast of tumor in SET2 and TSEfs is better than in other fast images. Respiratory artifacts in TSE images are greater than in SET2 and other fast images.

Breath-hold T2 weighted imaging of liver

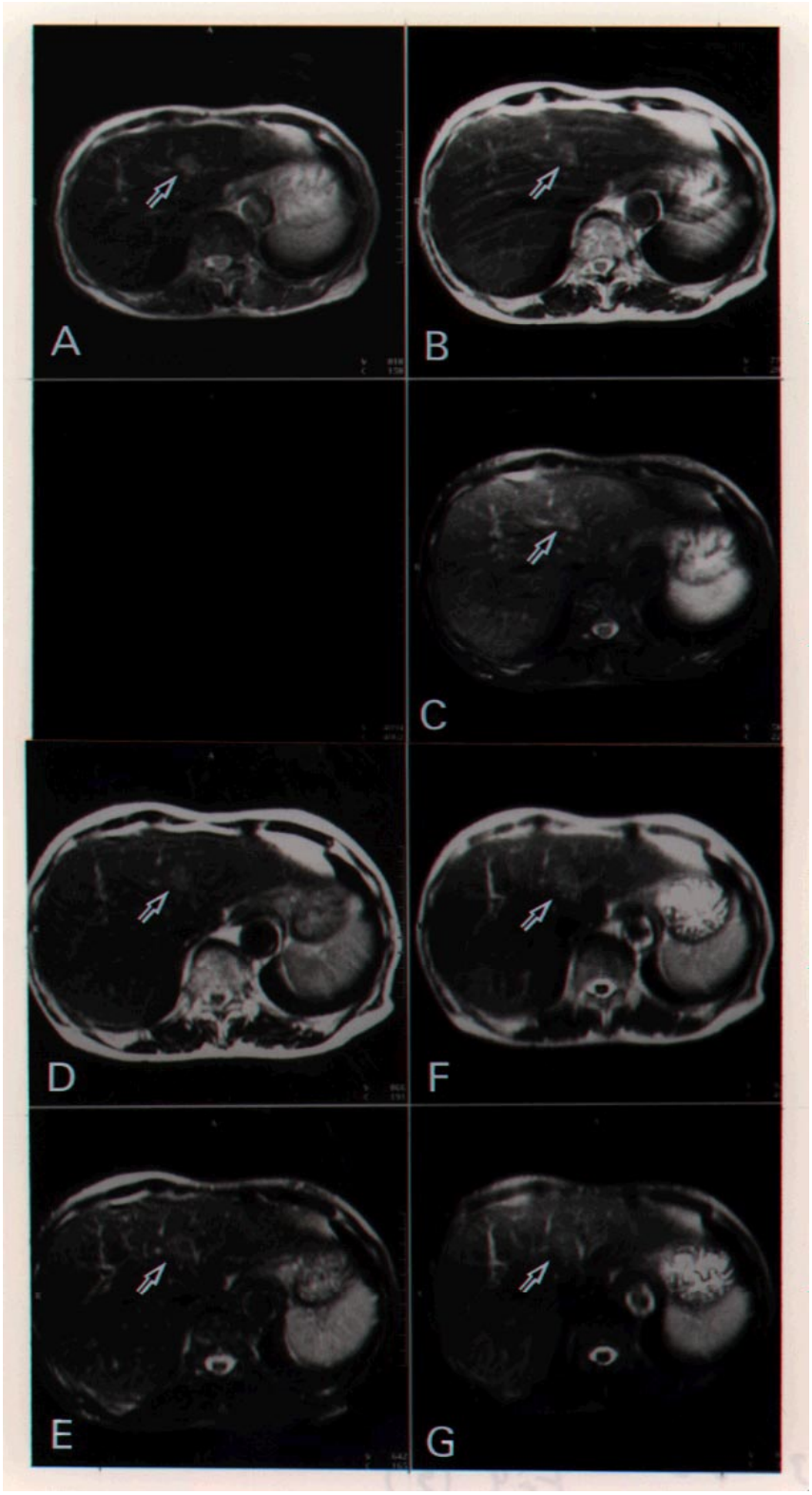

Table 3. Detectability of tumorous lesions on fast, chemical fat-saturation fast and conventional T2-weighted spin-echo MR images

Sequence	Tumor size (cm)				
	1 cm <	≤ 1-2 cm <	≤ 2-3 cm <	≤ 3 cm	Total
SET2	4 (3)	9 (1)	11 (1)	9	33 (5)
TSE	5 (1)	8 (1)	10 (1)	10	33 (3)
TSEfs	4 (1)	8 (1)	10 (1)	9	31 (3)
BH-TSE	2 (1)	6 (1)	10 (1)	10	28 (3)
BH-TSEfs	2 (1)	5 (1)	10 (1)	10	27 (3)
HASTE	4 (1)	9 (1)	7 (1)	10	30 (3)
HASTEfs	4 (1)	9 (1)	7 (1)	10	30 (3)

( ), cyst.
The abbreviations are the same as in Tables 1 and 2.

about 1 s by producing 180 pulses 128 times per each excitation pulse and phase-encoding of each echo (Hening et al., 1986; Fujii, 1994). However, TSE has been reported to differ from SE in that it is affected markedly by the magnetization transfer contrast (MTC) effect, that the susceptibility effect is small, and that edge enhancement effect is obtained (Wolf and Balaban, 1989; Melki and Mulkem, 1992). The contrast of TSE images is also reported to be altered by changes in the number of echo factors. In HASTE, also, echoes near the end of the pulse series are weakened in tissues with short T2 due to attenuation of T2 during data accumulation, and the resolution in the phase-encoding direction is reduced (Catasca and Mirowitz, 1994; Outwater et al., 1994).

In quantitative evaluation, the liver SNR was slightly lower in TSE and BH-TSEfs images, but was similar to or higher in other methods than in SET2. Especially, the SNR was significantly higher in TSEfs, the CNR_T was significantly higher in HASTE, and both SNR and CNR_T were significantly higher in HASTEfs than in SET2. In TSE, the signals of adipose tissue are higher in SET2 so that artifacts of the abdominal wall associated with respiratory motions are stronger, and the noise is greater. This is probably why the SNR of the liver was slightly lower. In TSEfs, noise was reduced by fs, and liver signals were higher than in SET2 because of 5 signal acquisitions. Therefore, the SNR of the liver was significantly higher than in SET2, unlike TSE. Also, the CNR_T was significantly higher in TSEfs images than in TSE images, probably because tumor-liver contrast was increased by fs with a resultant decrease in noise.

In BH-TSE with only 1 signal average, the MTC effect was increased with a boost in the number of echo factors, and fat signals were intensified in relative terms as compared with TSE, hence low liver signals. In addition, it required 23-s breath holding, and the images were markedly deteriorated if breath-holding was insufficient. However, repetition time (TR) and effective echo time (TE) were sufficiently longer than in SET2 with resultant enhancement of T2-weighting. Therefore, the SNR of the liver was lower, but the CNR_T was higher than in SET2 although the differences were not significant.

In HASTE, the imaging time was 14 s (1 s/shot) so that sufficient breath-holding was possible in nearly all patients. Therefore, no deterioration of the image quality due to respiratory artifact was observed, and background noise was low. Since T2 relaxation has nearly been complete in most tissues in the latter part of the echo train, intense T2-weighted images can be obtained. Also, as each slice is obtained as a single shot by this method, the MTC effect of neighboring slices can be ignored. For these reasons, the CNR_T was significantly higher in HASTE, and the SNR of the liver and CNR_T were significantly higher in HASTEfs than in SET2 or TSE.

The results of the qualitative evaluation generally reflected those of the quantitative evaluation. In TSE, respiratory artifacts were significantly higher, but the TR and effective TE were longer, so that the visibility of the tumor was excellent. TSEfs, in which respiratory artifacts are reduced by fs, were superior to SET2 in all evaluation items except for the sharpness of the liver margin. Of the breath-hold imaging techniques, artifacts were small, and visualization of the tumors and sharpness of the liver were excellent in BH-TSE, and HASTE was better in some items than SET2 due to small artifacts. However, no significant difference as compared with SET2 was observed in overall quality because of the low contrast resolution of the tumor due to the MTC effect in BH-TSE and because of the low spatial resolution in HASTE.

Concerning the detectability of tumors, SET2 was better than the fast imaging methods. But one node in the lower margin of the liver, where respiratory movement is prominent, was not visualized. Because of the strong respiratory artifacts in TSE, the low contrast resolution of the tumor due to the MTC effect in BH-TSE, and the low spatial resolution in HASTE, the detectability of the fast imaging methods were low.

Conclusion

Fast T2-weighted MRI of liver tumors including breath-hold scanning techniques is inferior to SET2 in the detectability of tumors and is not considered to replace completely SET2 as a diagnostic procedure despite its quantitative and qualitative advantages.

References

1 Catasca JV, Mirowitz SA. T2-weighted MR imaging of the abdomen: fast spin-echo vs conventional spin-echo sequences. AJR Am J Roentogenol 1994;162:61–67.

2 de Lange EE, Mugler JP, Bosworth JE, DeAngelis GA, Gay SB, Hurt NS, et al. MR imaging of the liver: breath-hold T1-weighted MP-GRE compared with conventional T2-weighted SE imaging-lesion detection, localization, and characterization. Radiology 1994;190:727–736.

3 Egglin TK, Rammeny E, Stark DD, Wittenberg J, Saini S, Ferruci JT. Hepatic tumors: quantitative tissue characterization with MR imaging. Radiology 1990;176:107–110.

4 Feinberg DA, Oshio K. GRASE (gradient- and spin-echo) MR imaging: a new fast clinical imaging technique. Radiology 1991;181:597–602

5 Fujii K. Fast imaging technique in MRI. Gazo Shindan 1994;14:55–71 (in Japanese).

6 Haase A, Frahm J, Haenicke W. H NMR chemical shift selective (CHESS) imaging. Phys Med Biol 1985; 30:341-344.

7 Hata Y, Tada S. Fat suppression techniques. Gazo Shindan 1994;14:48–54 (in Japanese).

8 Hening J, Nauerth A, Friedburg H. RARE imaging: a fast imaging method for clinical MR. Magn Reson Med 1986;3:823–833.

9 Jones KM, Mulkem RV, Schwartz RB, Oshio K, Bames PD, Jolez FA. Fast spin-eho MR imaging of the brain and spine: current concepts. AJR Am J Roentogenol 1992;158:1313–1320.

10 Melki PS, Mulkem RV. Magnetization transfer effects in multi-slice RARE sequences. Magn Reson Med 1992;24:189–195.

11 Nghiem HV, Herfkens RJ, Francis IR, Sommer FG, Jeffrey RB, Li KCP, et al. The pelvis: T2-weighted fast spin-echo MR imaging. Radiology 1992;213–217.

12 Outwater EK, Mitchell DG, Vinitski S. Abdominal MR imaging: evaluation of a fast spin-echo sequence. Radiology 1994;190:425–429.

13 Rammeny E, Weissleder R, Stark DD, Saini S, Compton CC, Benett W, et al. Primary liver tumors: diagnosis by MR imaging. AJR Am J Roentogenol 1989;152:63–72.

14 Rydberg JN, Lomas DG, Coakley KJ, Hough DM, Ehman RL, Riederer SJ. Comparison of breath-hold fast spin-echo pulse sequences for T2-weighted MR imaging of liver lesions. Radiology 1995;194:431–437.

15 Siewert B, Muller MF, Foley M, Wielopoiski PA, Finn JP. Fast MR imaging of the liver: quantitative comparison of techniques. Radiology 1994; 193:37-42.

16 Stalk DD, Hendrick RE, Hahn PF, Ferrucci JT. Motion artifact reduction with fast spin-echo imaging. Radiology 1987;164:183–191.

17 Taupitz M, Spidel A, Hamm B, Deimling M, Reichel M, Bock A, et al. T2-weighted breath-hold MR imaging of the liver at 1.5 T: results with a three-dimensional steady-state free procession sequence in 87 patients. Radiology 1995; 194:439–446.

18 Winkler ML, Thoeni RF, Luh N, Kaufmann L, Margulis AR. Hepatic neoplasia: breath-hold MR imaging. Radiology 1989;170:801–806.

19 Wolf SD, Balaban RS. Magnetization transfer contrast (MTC) and tissue water proton relaxation in vivo. Magn Reson Med 1989;10: 135–144.
20 Wood ML, Runge VM, Henkelman RM. Overcoming motion in abdominal MR imaging. AJR Am J Roentogenol 1988;150:513–522.
21 Yosida K, Suto Y, Kato T, Sugihara S, Ohmura N. Evaluation of fast gradient system breath-hold FLASH imaging in the examination of liver tumors: comparison with conventional spin-echo pulse sequences. Yonago Acta Med 1996;39:73–81.

(Received August 19, Accepted September 26, 1996)